A comprehensive oceanographic dataset of a subpolar, mid-latitude broad fjord: Fortune Bay, Newfoundland, Canada

Sebastien Donnet[1], Pascal Lazure[2], Andry Ratsimandresy[1], Guoqi Han[1,3]

[1] Fisheries and Oceans Canada, Northwest Atlantic Fisheries Centre, 80 East White Hills Rd, St. John's NL, A1C 5X1, Canada
[2] Ifremer (French Research Institute for Exploitation of the Sea) Laboratoire d'Océanographie Physique et Spatiale, Centre Bretagne, ZI de la Pointe du Diable, CS 10070, 29280 Plouzané, France
[3] Fisheries and Oceans Canada, Institute of Ocean Sciences, PO Box 6000, Sidney BC, V8L 4B2, Canada

Correspondence to: Sebastien Donnet (sebastien.donnet@dfo-mpo.gc.ca)

Abstract. While the dynamics of narrow fjords, i.e. narrow with respect to their internal Rossby radius, have been widely studied, it is only recently that interest sparked in studying the physics of broad fjords due to their importance in glacial ice melting (in Greenland, especially). Here, we present a comprehensive set of data collected in Fortune Bay, a broad, mid-latitude fjord located on the Northwest Atlantic shores. Aside from being wide (15 - 25 km width) and deep (600 m at its deepest), Fortune Bay also has the characteristics of having steep slopes, weak tides and of being strongly stratified from spring to fall. Thus, and since strong along-shore winds also characterise the region, this system is prone to interesting dynamics, generally taking the form of transient upwelling and downwelling travelling along its shores, similar to processes encountered in broad fjords of higher latitudes. The dataset collected to study those dynamics consists of water column physical parameters (temperature, salinity, currents and water level) and atmospheric forcing (wind speed and direction, atmospheric pressure, air temperature and solar radiation) taken at several points around the fjord using oceanographic moorings and land-based stations. The program lasted 2 full years and achieved a good data return of 90%, providing a comprehensive dataset not only for Fortune Bay studies but also for the field of broad fjord studies. The data are available publically from the SEANOE repository (https://www.seanoe.org/data/00511/62314/; Donnet and Lazure, 2020).

1 Introduction

Fortune Bay is a broad fjord-like embayment located on the south coast of Newfoundland, a large island of the Northwest Atlantic (Figure 1). It is about 130 km long and 15-25 km wide, with a maximum depth of about 600 m. It is semi-enclosed from the shelf by a series of sills of about 100-120 m limiting depth. While situated in mid-latitudes (about 47°N) the marine climate of this region can be defined as subpolar due to the cooling effect of the cold, equatorward Labrador Current of arctic origin (Dunbar, 1951 and Dunbar, 1953). As a result, its waters are strongly stratified in summer (de Young, 1983, Donnet et al., 2018a) and its internal Rossby radius Ri is smaller than its width (Ri ~5-10 km), making it similar to large polar fjords in that regard (e.g. Cottier et al., 2010).

While dynamics of narrow fjords, i.e. narrow with respect to their internal Rossby radius, have been well studied, wide fjords dynamics are much less known (see Farmer and Freeland 1983, Inall and Gillibrand 2010 and Stigebrandt 2012 for reviews of narrow fjords). Similarly to narrow fjords, and to any coastal areas, tides, winds, freshwater input and remote forcing (e.g. pycnocline and sea-level differences with shelf water) all play a role in the dynamics of broad fjords (e.g. see Cottier et al., 2010 for a review). However, having a width larger than their internal Rossby radius allows for each side to behave independently or have important 'wall-to-wall' effects (e.g. Cushman-Roisin et al., 1994, Jackson et al., 2018). In other words, rotation induces cross-fjord variations, in stratification and/or flow, such as surface freshwater distribution, deep water flow and potential transient wind-induced upwelling/downwelling events (Cottier et al., 2010).

Due to their importance in climate change studies, interest in wide fjords such as those present in Greenland has grown in recent years (e.g. Straneo and Cenedese, 2015, Inall et al. 2015, Jackson et al. 2018). Nevertheless and due to their remoteness, available observational data for those important regions remains very scarce.

The first set of oceanographic studies dedicated to Fortune Bay was conducted by researchers and students of Memorial University of Newfoundland (MUN) from the late 1980s to the mid-1990s and focused on deep-water dynamics (de Young and Hay 1987, Hay and de Young 1989 and White and Hay 1994) as well as its lower trophic biology (Richard, 1987 and Richard and Haedrich, 1991). Later on and with the development of the aquaculture industry in the region, renewed interest led to new studies focusing on general geographic and oceanographic characteristics (Donnet et al., 2018b), hydrography (Ratsimandresy et al., 2014, Donnet et al., 2018a), ocean currents (Ratsimandresy et al., 2019) as well as more specific dynamics induced by strong wind events (Salcedo and Ratsimandresy, 2013). Based on these latter studies, which focused on the inner part of the embayment, it became evident that a comprehensive and large-scale (i.e. bay scale) survey would be necessary to understand the dominant dynamics of this region.

To this end, an observation program took place from May 2015 to May 2017. The program was centered on the deployment and recovery of oceanographic moorings, deployment and recovery of weather stations and tide gauges and on the collection of temperature and salinity profiles (Figure 1). The key objective and feature of this program was to measure the water column stratification and currents simultaneously at multiple sites, continuously through the four seasons. Along with the observations, a numerical model is being implemented to help understand the processes involved and to predict the transport of variables of interest (e.g. virus, sea-lice or organic material originating from or going into aquaculture farms). The main objective of this paper is to report on the data products, describing the methods, limitations, estimated uncertainties and main results in the hope of being useful not only to further studies of the region but also more generally to the field of broad fjord dynamics studies. The dataset and its summary description are available at: https://www.seanoe.org/data/00511/62314/.
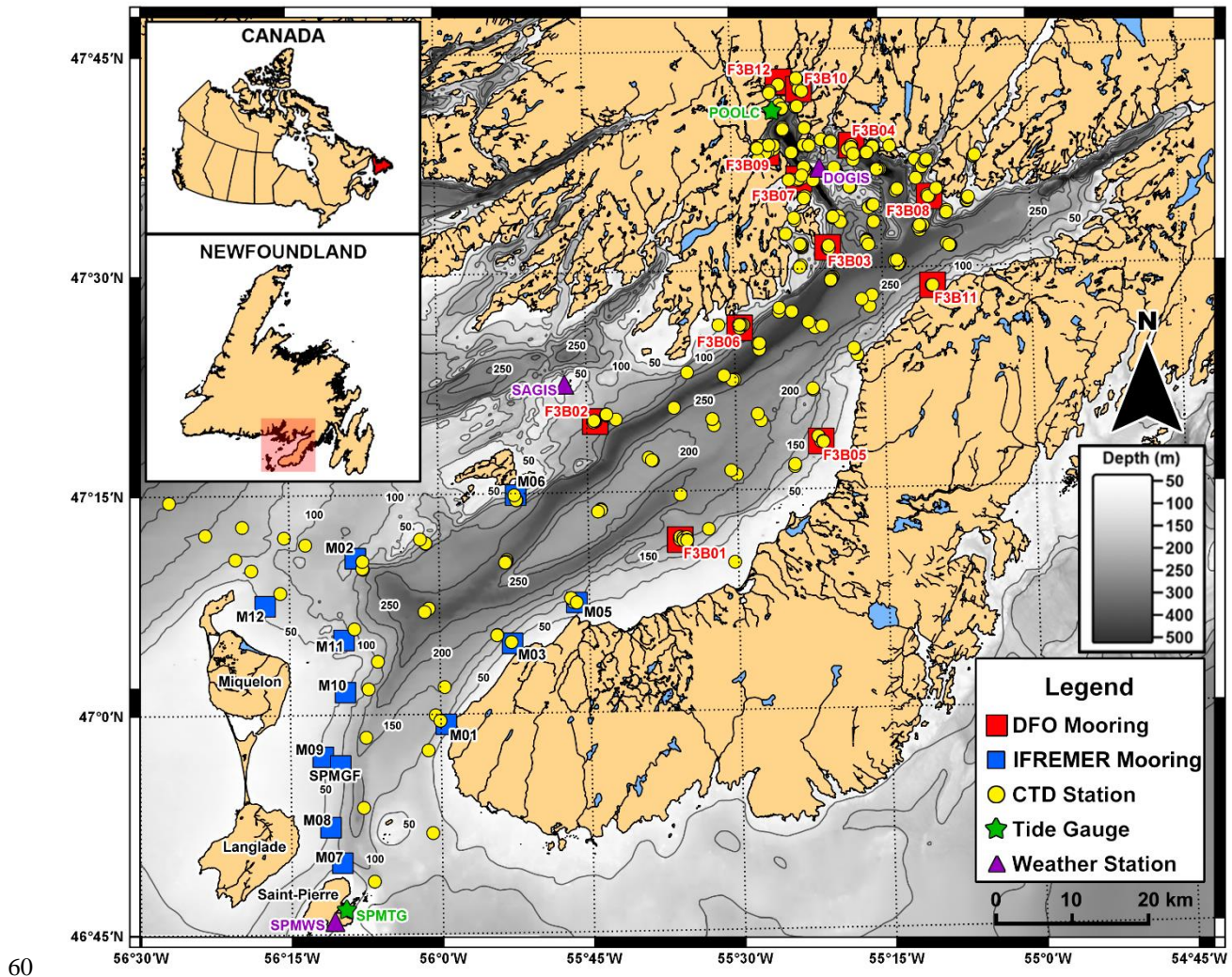
60

Figure 1: Study area and summary of the observation program (May 2015 – May 2017)

2 Material & methods

The observation program started in May 2015 with the deployment of 8 moorings at 4 sites (F3B01-04), a weather station (DOGIS) and a tide gauge (POOLC). The program lasted for two full years (May 2015 – May 2016 defined herein as 'year 1'

65 and May 2016 – May 2017 defined herein as 'year 2') with maintenance trips occurring every 6 months. Thus, field operations occurred in May and November of each year for about 10-15 days each time; delimiting 4 observation periods defined herein as 'leg': May-November 2015 (leg 1), November 2015 – May 2016 (leg 2), May-November 2016 (leg 3) and November 2016 – May 2017 (leg 4). During each trip, additional measurements consisting of CTD (Conductivity, Temperature and Depth) profiles were collected and a separate trip was organised in August 2016 to get a better seasonal picture of the temperature and

70   salinity field over the whole region. A small opportunistic survey, restricted to Belle Bay area, also occurred in June 2016 during the re-deployment of mooring F3B08.

The moorings consisted of a string of thermistors mounted with a couple of CTDs (one within each main hydrographic layer) and one (year 2) or two (year 1) ADCPs (Figure 2). The setup changed from year 1 to year 2 by merging the originally separated ADCPs and thermistor-CTDs lines (by about 100-150 m); thereby doubling the amount of main sites being monitored from 4

75   (F3B01-04) to 8 (F3B01-08). Two other moorings lines were added, F3B09&10 and F3B11&12 for leg 3 and 4, respectively, to further increase the spatial resolution. With the exception of 2 moorings during leg 1 (F3B01&02), all moorings were sub-surface, taut-line type. A surface spar buoy was used during leg 1 on F3B01&02 in an attempt to measure near-surface conditions and as a deterrent to fishing and shipping activities. The experiment was, however, unsuccessful with the loss of both surface buoys after about 5 months deployment due to wave action wearing the mooring lines. Of those surface

80   measurements, only one CTD dataset was partially recovered (RBR#60134 from F3B01, found on the shore with its spar buoy). Two main types of mooring were used during year 1 (Figure 2), an "ADCP" type having a set of two upward-looking ADCP separated by a string of thermistors and a "CTD" type consisting of two CTDs separated by a string of thermistors. The CTD type was declined in two version for leg 1: surface (F3B01&02) and sub-surface (F3B03&04). For leg 2, only the subsurface version was retained; adding a 9 m rope on the top part of F3B01&02. In year 2, the "CTD" mooring design of year

85   1 was used as a base and equipped with an ADCP on the bottom part (around 80 m) to combine water stratification with ocean currents measures for most of the sites (F3B01-08). On F3B09 and 10, a simpler design was used due to the shallower depth of the sites, a need for less buoyancy and limitation on available hardware. To minimize drag we used ¼" dyneema ropes and OpenSeas SUBS buoys (Hamilton et al., 1997). CTDs were mounted in stainless-steal cages for protection and thermistors were simply attached on the rope using cable ties and electrical tape. In most cases, acoustic releases were mounted in tandem

90   for redundancy. Cooperation with our partner IFREMER (Institut Français de Recherche pour l'Exploitation de la MER) resulted in other sites being equipped with either bottom mounted thermistor (M01-10 Mastodon, Lazure et al., 2015) or ADCP moorings (SPMGF) during some of the legs (leg 3 for M01-10 and all along for SPMGF).
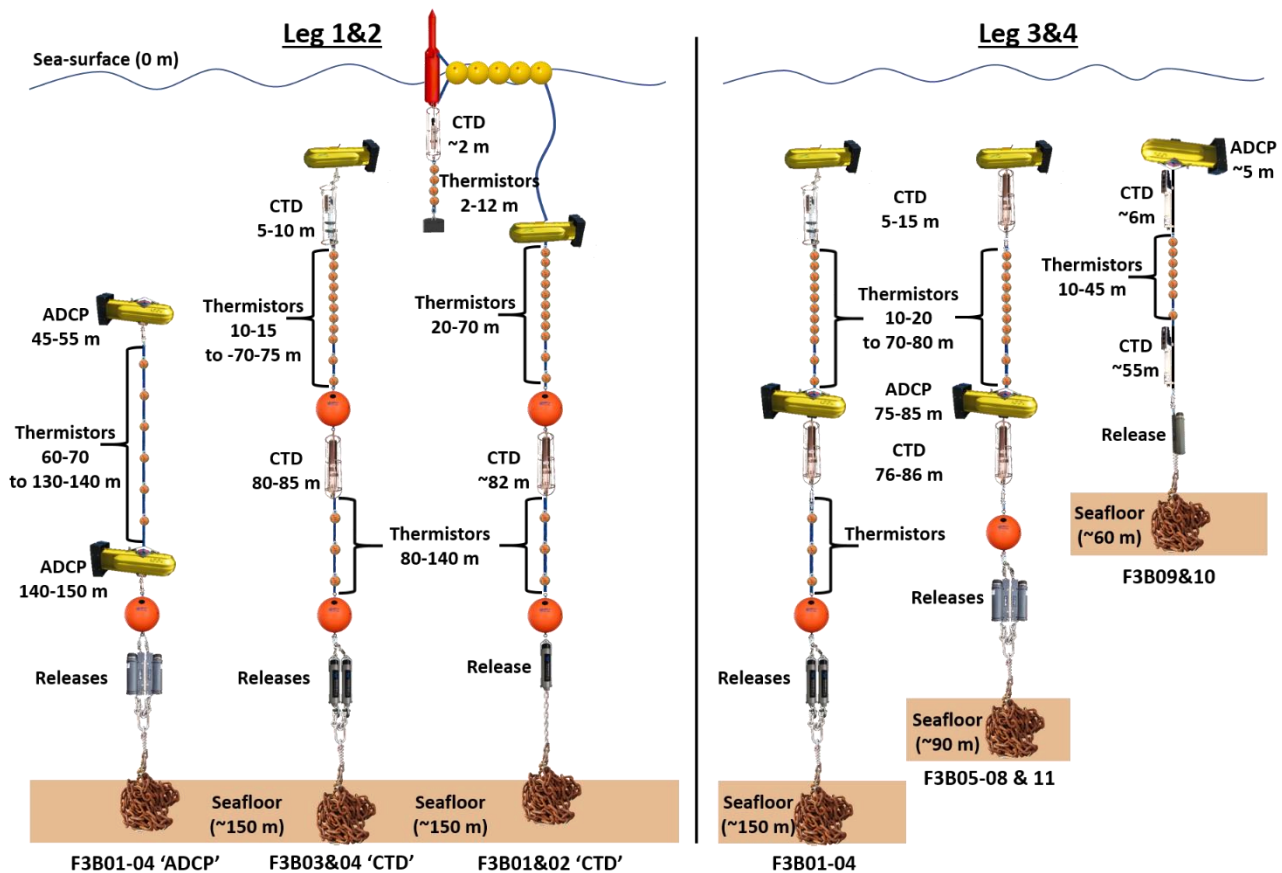
Figure 2: DFO taut line moorings, leg1&2 (left), leg 3&4 (right). In leg 2, F3B01&2 'CTD' lines were converted to F3B03&04's design due to failures of the sea-surface part. A 110 m rope, without thermistors, was added under the bottom CTD of F3B08 to be deployed

The other fixed (and long-term) structures were land-based and consisted of a weather station measuring wind speed and direction (at 2 m and 10 m height above ground) as well as barometric pressure, air temperature, solar radiation (Qs) and Photosynthetically Active Radiation (PAR) and of a tide gauge measuring the sea level and sea surface temperature. Two weather station structures were installed on a small, barren island (DOGIS, see Figure 1 for location and Appendix A for an illustration): a 2 m height tripod on which was mounted a wind sensor, a barometer, a temperature sensor, a pyranometer (i.e solar radiation sensor) and PAR sensor and a 10 m mast on which was mounted another wind sensor. The tide gauge was installed on a wooden wharf at the head of the bay (POOLC, see Figure 1 for location and Appendix A for an illustration) and equipped with a vented pressure sensor mounted below chart datum in a black PVC tube to limit biofouling. These atmospheric and tide observations completed existing sites equipped by other agencies (Figure 1): Sagona Island (SAGIS) weather station (Environment and Climate Change Canada), St Pierre airport weather station (Meteo France) SPMWS, and St Pierre harbour tide gauge (Service hydrographique et océanographique de la Marine, France) SPMTG.

2.1 Instruments used

110 A variety of instruments was used during this program, selected for their proven and common use in the field of physical oceanography and atmospheric science. All our ADCPs were WorkHorse models (WH) from Teledyne RDI (T-RDI); most of them were 300 kHz type though a few 600 kHz and one 1200 kHz (WH300, WH600 and WH1200, respectively) were also used during the second year. Most of the CTDs were SeaBird Electronic (SBE) instruments, model 19 ('SeaCAT' manufactured in the 90s) with a few 37 ('microCAT' manufactured in the 2000s). A few RBR concerto CTDs as well as

115 XR420 Temperature-Depth-Dissolved Oxygen instruments were used on some legs (typically as backup and/or complementary observations). All the thermistors used were disposable Onset HOBO TidBiTs (UTBI) and a few Onset HOBO U20 thermistors equipped with a pressure sensor were also used to complement the UTBI and provide additional depth information of the mooring line. Gill windsonic sensors were used on our weather stations to measure wind speed and direction and were plugged to an Onset HOBO U30 logger on the 2 m tripod and to a Sutron SatLink2 logger with real-time transmit

120 capability on the 10 m mast. An Onset Smart Barometric Pressure Sensor barometer (model S-BPA-CM10), an Onset 12-Bit Temperature Smart Sensor air temperature sensor (model S-TMB-M002), an Onset Silicon Pyranometer Smart Sensor (S-LIB-M003) and an Onset PAR Smart Sensor (S-LIA-M003) were also mounted on the 2 m tripod. A Sutron submersible pressure transducer (model 56-114) was used for the tide gauge; plugged to a Sutron SatLink2 logger with real-time transmit capability. Characteristics and specifications of all the sensors used are provided in Table 1.

2.2 Instruments limitations and uncertainties

125

Due to their difference in memory and battery capacity, sampling strategy (i.e. interval) differed from one instrument to another. All the ADCPs were set to sample every 30 min during leg 1-3. For leg 4, a higher sampling rate of 5 min was chosen to increase temporal resolution on moorings F3B03-12. In year 1, ADCPs were setup in 'burst mode', that is sampling for a smaller amount of time than their sampling interval (7.5 min vs. 30 min) to avoid possible cross-talk interference since two

130 instruments of the same frequency were used on the same line. In year 2, all the ADCPs were sampling evenly (i.e. continuously) along the sampling average period. Higher vertical resolution (1 m cell) and broadband mode were used during leg1&2 for the near-surface units while lower vertical resolution (3m cell) and narrowband mode was used for the near-bottom units to maximise range. Overall, a reduction of about 30% in profile range from the manufacturer specifications was found due to the clarity of the water (i.e. low backscattering volume conditions). Based on first year results, the sampling strategy

135 was re-thought to increase the horizontal sampling in year 2 (8 or more sites vs. 4) while keeping vertical profiling of the stratified part of the water column. i.e. from about 10 m to 80 m depth. Cell size was increased from 2 m (leg 3) to 3 m (leg 4) to prevent from losing range during very clear water conditions usually observed in winter. Narrowband mode was used for all our units during year 2 for the same reason.

SBE & RBR CTDs were all set to sample at 20 min interval while the XR420 were set at 1 min interval during leg 2 and 20

140 min during leg 3&4. The UTBI were set to 10 min interval along with the SUTRON weather station and tide gauge (with a 1

min internal average for the SUTRON). The U30 weather station was initially setup with a 30 min interval with no averaging during leg 1&2 and then adjusted to a 10 min interval, 30 samples averaged, during leg 3&4.

145 **Table 1: instrumentation used, sampling setup and stated uncertainty (i.e. noise) based on manufacturer specification and sampling setup. "top" and "bottom" refers to ADCP position on the mooring line during Leg1&2 (about 50 m vs. 145 m depth, respectively).**

Instrument	Sampling Interval (# sample averaged)	Uncertainty
T-RDI ADCPs	30 min (120) – Leg1&2 top 30 min (60) – Leg1&2 bottom 30 min (200) – Leg 3 30 min (200) – Leg 4 F3B01-02 5 min (33) – Leg 4 F3B03-12	0.7 - 1.7 cm/s 0.03 - 0.07 ºC 1.4 - 3.5 cm
SBE19 CTDs	20 min (1)	0.01 ºC 0.02 (Salinity) 10 - 30 cm (unit dependant)
SBE37 CTDs	20 min (1)	0.002 ºC 0.006 (Salinity) 2% (DO) 1 cm
RBR Concertos	20 min (60)	0.0003 ºC 0.0008 (Salinity) 1.3 cm
RBR XR420	1 min (1) – Leg 2 20 min (60) – Leg 3&4	0.0004 - 0.002 ºC 2% (DO) 4.6 - 25 cm
HOBO UTBI	10 min (1)	0.21 ºC
HOBO U20	15 min (1)	0.44 ºC 12 cm
Mastodon	1 min (1)	0.1 °C
HOBO U30	30 min (1) – Leg 1&2 10 min (30) – Leg 3&4	0.4 - 2 % wind speed 0.5 - 3 º wind direction

		0.9 - 5 mbar (atmospheric pressure)
		0.04 - 0.2 ºC (air temperature)
		12 - 64 W/m^2 (solar radiation)
		40 - 125 umol/m^2/s (PAR)
HOBO U20 (weather station)	15 min (1)	0.44 ºC (air temperature)
		12 mbar (atmospheric pressure)
SUTRON weather station	10 min (60)	0.3 % wind speed
		0.9 º wind direction
SUTRON tide gauge	10 min (1)	0.3 cm
		1 ºC

2.3 ADCP backscatter processing

To provide with some added value, the ADCP backscatter data were processed to convert the raw Returned Signal Strength Indicator (RSSI, E in equation below), a measure of acoustic pressure received by the transducers, to a corrected backscatter volume Sv, proportional to the amount (i.e. volume) of particles present in the water column. The method used to do the correction is an updated version of the popular Deines' method (Deines, 1999) published by Mullison (2017) and summarized by this equation (Mullison 2017, eq. 3):

$$Sv = C + 10\log((Tx+273.16)R^2) - 10\log(L_{DBM}) - 10\log(P_{DBW}) + 2aR + 10\log(10^{Kc(E-Er)/10} - 1)$$

Factory calibrated values of Kc (count to decibel factor) and Er (noise floor) were used to solve this equation, along with the temperature measured at the transducer head by the instrument (Tx). Transducer temperature measured at transducer head and salinity value selected during instrument setup (ES command; 32 in our deployments) were used to calculate the water absorption (a) along the range (from transducer) R; thereby implying homogeneous water conditions. The transmit pulse length L_{DBM} was calculated using bin size (1-3 m) and beam angle (20º) values. Default values of constant C and transmit power P_{DBW} provided by Mullison (2017, table 2) were used.

Overall, a combined uncertainty of 5 dB is estimated due to the assumption of water column homogeneity (constant absorption, 0.5 dB maximum error in summer toward the surface), the assumption of constant power source (±3 dB with alkaline batteries, reducing in transmit power with time) affecting Leg1&2 ADCPs more than Leg3&4 ADCPs which were using lithium batteries (featuring a quasi-constant transmit power all along a deployment) and inherent transducer linearity uncertainties (±1.5 dB according to Deines, 1999). This uncertainty is relatively small in comparison to the 55 dB average range (-90 to -35) observed along the program, i.e. less than 10%, though not negligible. Note that this uncertainty can be qualified as being 'relative' in a

sense that it is an uncertainty applicable to any given timeseries taken separately. In absolute terms, bias can exist due to the assumption made on the constants C and P_{DBW} which may differ from one instrument to another.

3 Results

In total, 40 ADCP timeseries, 60 CTD/TD-DO timeseries (33 SBE19, 16 SBE37, 6 RBR XR420 and 5 RBR concerto), 35 UTBI string series, 13 U20 timeseries, 11 Mastodon thermistor series, 16 weather station series (6 U30, 6 SUTRON and 4 U20) and 4 tide gauge series were collected (Appendix B, Table B-1 to Table B-6). Taken together, these timeseries amount to about 28715 record-days (about 79 years).

Percent coverage presented in Appendix B (Table B-1 to Table B-6) are calculated based on the recovered instruments and data only. Lost instrument or instrument from which no data could be recovered is not presented. In total: 1 CTD was lost (RBR#60135 on F3B02, Leg 1), 1 CTDs flooded without any possible data recovery (SBE19#1310 on F3B04 leg 2) and 14 UTBI were lost (5 on F3B01-CTD leg 1, 5 on F3B02-CTD leg 1, 1 on F3B02-ADCP leg 2, 2 on F3B02-CTD leg 2 and 1 on F3B01 leg 3). Outside the failure of F3B01&02 top mooring part (10 units lost at once), UTBI were typically lost during grappling operations when releases could not be triggered. There were also one failed deployment attempt at F3B08 during Leg 3 (acoustic release failure in May 2016) which was successfully re-deployed in June 2016 but resulted in about 30 days of observation time lost (from early May to early June).

Percent coverages were calculated based on the good data recovery of current speed, current direction, current vertical speed and water column backscatter volume for the ADCPs; temperature, salinity and depth for the CTDs; temperature, dissolved oxygen and depth for the RBR TD-DO sensors; temperature and depth (or atmospheric pressure when used as a weather station sensor) for the U20s; temperature for the UTBIs; depth and temperature for the SUTRON tide gauge; wind speed and direction for the SUTRON weather station and wind speed, wind direction, atmospheric pressure, air temperature, PAR and solar radiation for the U30 weather station. For each instrument, the percent coverage represents the useable data covering the expected periods of observation; for a multiple parameters instrument (as listed above) the percent coverage was calculated for each parameter and then averaged per instrument.

Overall, the coverage is about 93% without considering instrument losses and about 91% when considering the losses. Illustrations of the data coverage are given in Figure 3 and Figure 4 as Gantt charts.
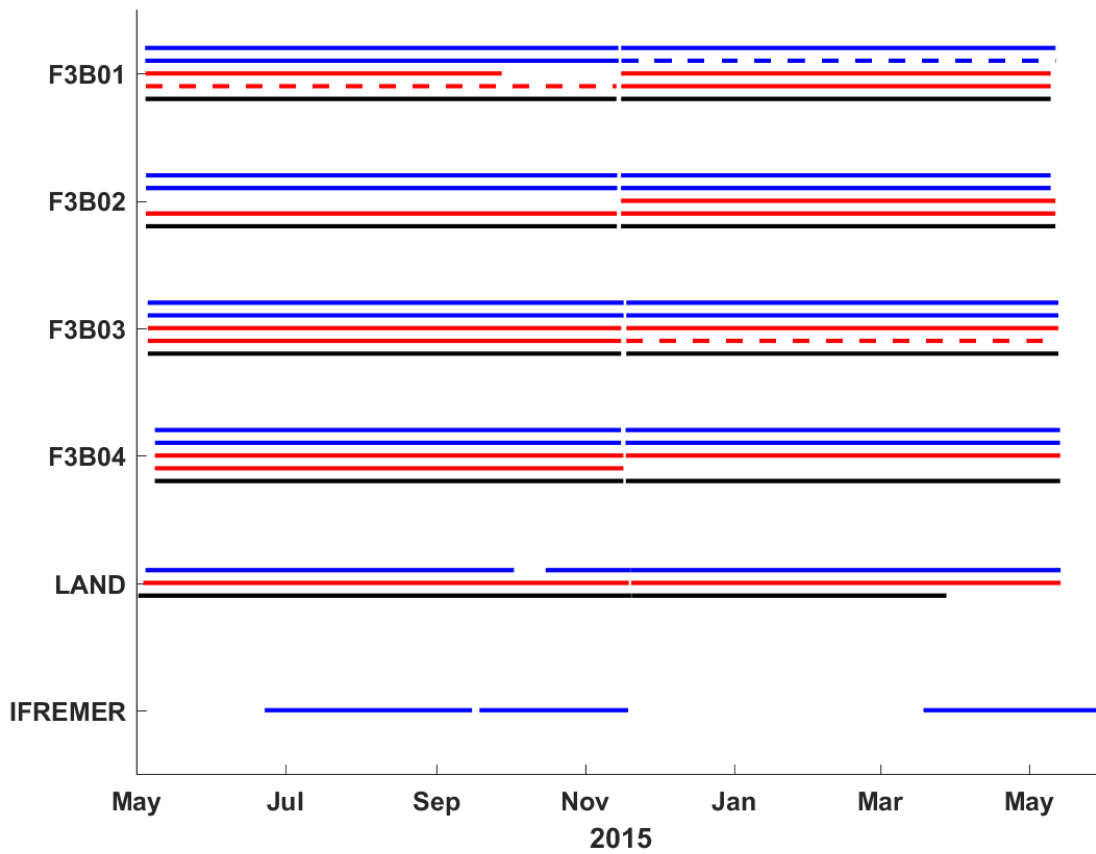
Figure 3: Data return, leg 1&2. For the moorings F3B01-04, ADCPs are in blue, CTDs are in red and UBTIs are in black. Top line correspond to the shallowest unit. For the land-based stations (LAND), DOGIS SUTRON weather station is in blue, DOGIS U30 weather station is in red and POOLC SUTRON tide gauge is in black. IFREMER ADCP data (SPMGF) is in blue. Dash lines represent partial data recovery (e.g. ADCP tilted, CTD having no or partial salinity return).

195
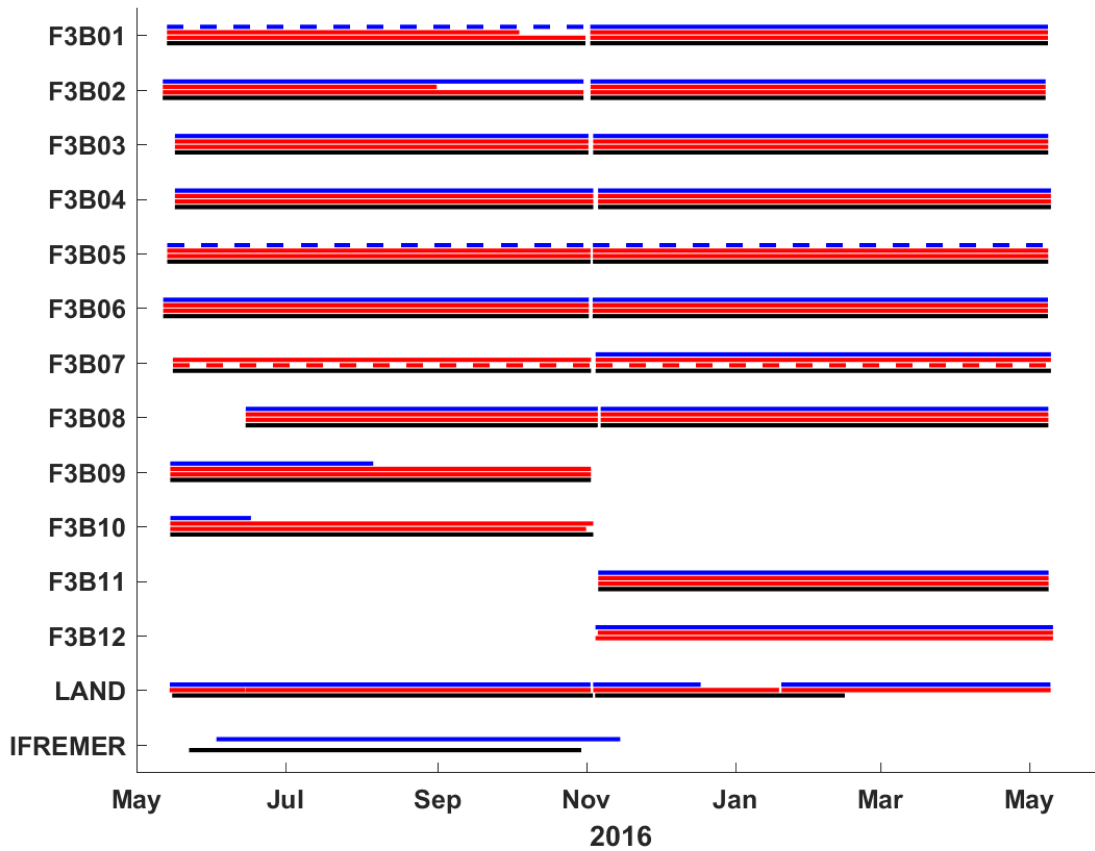
Figure 4: Data return leg 3&4. For the moorings F3B01-12, ADCPs are in blue, CTDs are in red and UBTIs are in black. Top line correspond to the shallowest unit. For the land-based stations (LAND), DOGIS SUTRON weather station is in blue, DOGIS U30 weather station is in red and POOLC SUTRON tide gauge is in black. IFREMER ADCP (SPMGF) and MASTODON (M01-12) data are in blue and black, respectively. Dash lines represent partial data recovery (e.g. ADCP tilted, CTD having no or partial salinity return).

4. Discussion

The primary objective of this observation program was to collect a robust baseline for studying the main physical processes affecting Fortune Bay. In particular, upwelling and downwelling propagations associated with strong currents along the shoreline were thought to be important features based on previous work done locally (Salcedo and Ratsimandresy, 2013, Donnet et al. 2018a) and in other embayments of the region (Yao 1986, de Young et al. 1993, Davidson et al. 2001, Ma et al. 2012). Hence, Fortune Bay's strong seasonal stratification, steep slopes, weak tides, strong along-shore winds and large width all indicated a potential for such 'coastally trapped' processes to occur.

The observation program was therefore designed to measure water vertical stratification and currents as well as forcing (i.e. wind and sea-level) over timescale of tens of minutes to a year-long and taken at as many locations as possible along the coast, within one internal Rossby radius, to follow potential disturbances travelling around the bay. Such features were indeed observed and an example of which is presented in Figure 5. The study of those features, including their generation, propagation, scale and importance on particles advection and water renewal, key aspects in studying the effect of aquaculture on the environment, will be the focus of future publications.

The uncertainty estimates presented in Table 1 are based on the instrument specifications and sampling strategy. That is, they represent the expected short-term (i.e. noise) fluctuation around the true measure and assume a perfectly calibrated instrument, i.e. no bias. Laboratory testing and in-situ performance checks were performed to further assess these estimates and correct for eventual bias. Laboratory testing were performed in a 3 m depth seawater tank (for the CTDs, mainly) to check temperature, salinity and depth measurements and a stable temperature water-bath was used to check temperature measurements (for the UTBI, mainly). In-situ checks were obtained using CTD casts taken just after deployment and right before recovery of the moorings and by cross-checking/comparing each instrument from the same mooring line (e.g. pressure measurements). The main biases found were with the pressure sensors of the moored SeaBird Electronic model 19 (SBE19) instruments, which could be as large as 6 dbar (~6 m of water depth). A combination of tank test results and in-situ check using the ADCP (and other instruments when available) and mooring line length were used to determine these pressure biases. Both pressure sensor data and corrected backscatter data (i.e. converted to volumetric backscatter values Sv in dB) were used to determine the in-situ depth of the ADCP (i.e. the distance to water surface when using backscatter values) which was then used to crosscheck the depth of the CTDs along the line. Biases that could not be determined with reasonable certainty resulted in discarding the data. Except for leg 1, each moored CTD was sent to the manufacturer for calibration prior to deployment. For leg 1, only laboratory tests could be done. All the thermistor used were new, i.e. bought for this program, and the ADCPs were 3-7 years old. The CTD profilers used were sent to the manufacturer for calibration on a yearly basis with a 3-year rotation scheme. i.e. 3 CTD profilers were available for this program and 1 profiler was sent per year to be used as a reference for the other 2 in laboratory and in-situ calibration/performance checks. Overall, it is estimated that the absolute depth of each instrument is known to the nearest meter, that the temperature is accurate at ±0.2ºC (UTBIs) or less (CTDs), that the salinity is within 0.1 (moored CTD) or less (CTD profiles) from the true value and that the current speed accuracy is ±2cm/s or better. Note that if further averaging were to be done on those original timeseries, the uncertainty would go down by the square root of the number of samples taken per sampling average except for the ±1m uncertainties on depth which can be seen as an unknown bias.
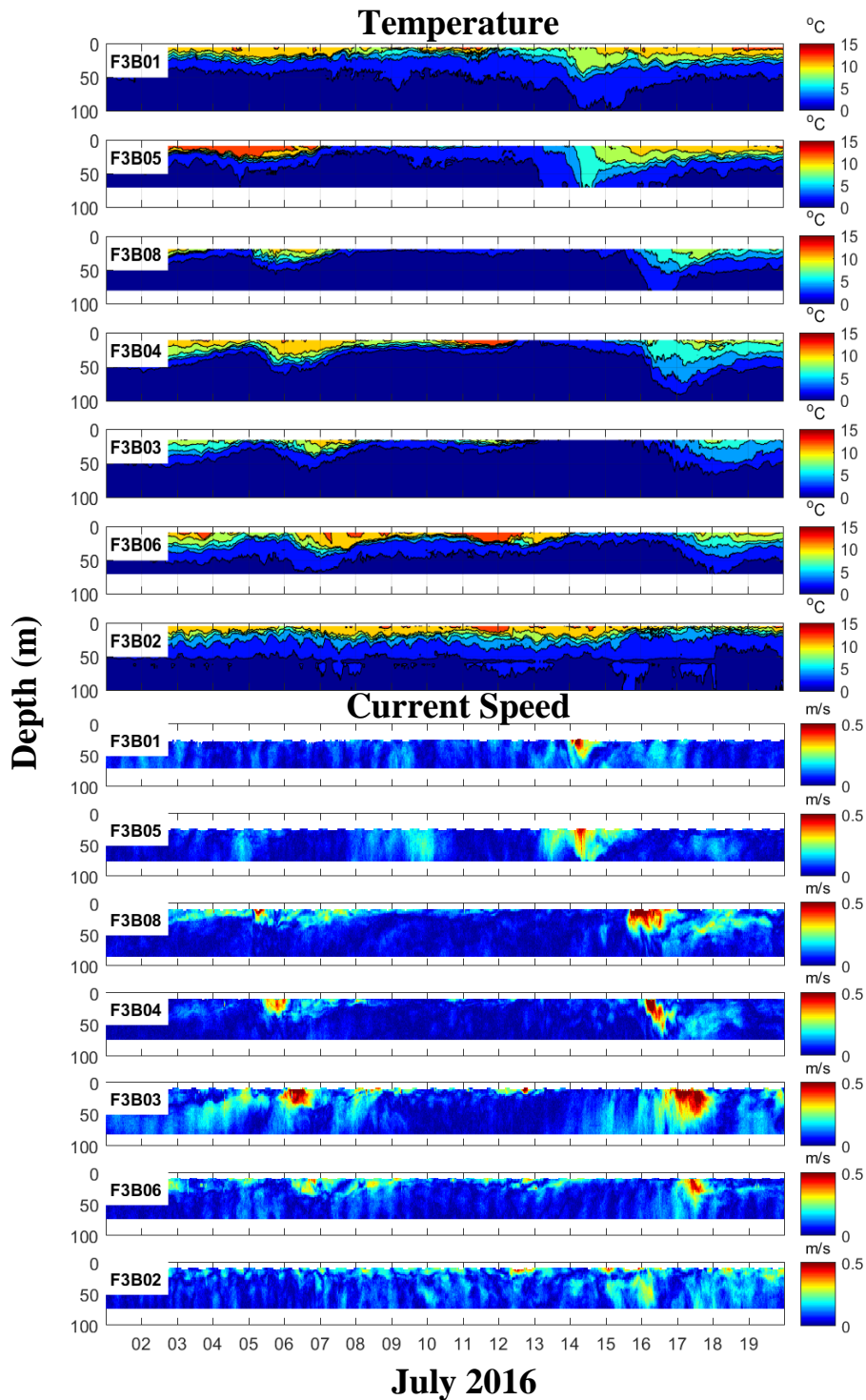
Figure 5: Fortune Bay water column thermal stratification and currents from July 1-20, 2016 showing several upwelling and downwelling events associated with strong currents 'pulses' travelling around the bay, i.e. from moorings F3B01 to F3B06.

4.2 Data limitations and issues

245 The program suffered from some instrument failures. ADCPs from F3B09&10 during leg 3 suffered from a battery failure (F3B09) and from a memory card failure (F3B10) resulting in data coverage of only 48% (slightly less than 3 months) and 17% (about 1 month), respectively. Two SBE19 CTDs (#1310 and #1312) got their electronic casing flooded resulting in a complete loss of data on F3B04, leg 2 (SBE19#1310) and in partial losses (small leak) on F3B03, leg 2, and on F3B07, leg 3&4 (SBE#1312, temperature and salinity data corrupted). The DOGIS SUTRON weather station suffered from a solar panel

250 failure during leg 1 resulting in a reduced coverage of 92% (a loss of about 12 days) and from a wind sensor failure during leg 3 (%56 coverage, a loss of about 33 days). DOGIS U30 weather station suffered from barometer issues during leg 1, 2 and 3 reducing coverages to 96%, 83% and 87%. The POOLC tide gauge also suffered from sensor failures, during both leg 2 and leg 4 of the program, resulting in reduced coverages of 73% (47 days lost) and 54% (86 days lost) and no coverage during the late winter-early spring seasons.

255 The program also suffered from some human errors and practical difficulties. Notably, several tangling of mooring ropes has resulted in excessive vertical tilt orientation of the upward-looking ADCP on moorings F3B01, 05 and 07 of leg 3 and on F3B05 leg 4, corrupting the data (see details below). In the case of leg 3 (F3B01, 05 and 07), problematic deployments in which the mooring line was not properly kept tight prior to releasing the anchor likely played a role. In the case of leg 4 (F3B05) it is less obvious since a stricter mooring deployment procedure was then in place and that field work records do not

260 indicate any wrong doing. The use of SUBS buoys, though improving mooring drag and potential 'knock-down' from strong currents, increases deployment difficulty when they are placed in the middle of a mooring line (as opposed to the top of a line) since they have a natural tendency of orienting themselves in the flow; thus, to have the rope close to their back fin when sinking downward, thereby increasing chances of being tangled. It should be noted that one case of tangling/excessive ADCP vertical tilt occurred to the bottom ADCP of F3B01 during leg 2, after about 3 weeks of deployment (see below for details and

265 Figure 7); thus not likely due to a deployment issue. Fishing activities may have caused it though no evidence of it could be found by looking at the data (e.g. rise and fall of the mooring); the data sampling frequency of the ADCP (30 min) prevents from a fine examination though no obvious evidence of mooring movement could be seen with the higher frequency UBTI records either (10 min) and fishing activities during that time of the year (December) is not very likely. The issue occurred during a strong current event, indicating that strong current shear could potentially be an actor.

4.3 QA/QC and data processing methods

270

Data were processed and quality checked similarly for all the instruments, that is:

1) raw data were first converted to the most convenient format known/available to the authors

2) time stamp and all variables of interest were extracted from the raw data and meta-data were associated to the dataset (i.e. station ID, geographical coordinates, deployment and recovery date and time and instrumentation ID)

275 3) using deployment and recovery time, 'out-of-water' data were removed

4) clock-drift and depth offset were assessed and corrected using concurrent data available on the same line. ADCPs were the most often used as a reference since their pressure sensor were systematically 'zeroed' prior to deploy and that their clock did not drift more than a few minutes per deployment. U20s and RBRs were usually used as a secondary reference or as a primary one when no ADCP were available on the same line (e.g. in leg 1&2). SBE19 units were the most affected by clock-drift and depth offset. A few units (SBE19 as well as UTBI) were also found to have been setup in local time instead of UTC, mistakenly.

5) 'out-of-range' data were removed using automatic filters following the criteria shown in Table 2. ADCP criteria was largely based on the manufacturer recommendations with current speed less than 0 (bad values are actually logged as -32768; see T-RDI documentation #P/N 957-6156-00, p147), Percent Good (PG) less than 25 (T-RDI documentation #P/N 957-6156-00, p150) and instrument tilt over 15 degree from the vertical (T-RDI documentation #P/N 957-6150-00, p17) used to remove bad data. Instrument vertical tilt was calculated using the pitch and roll records (see below for details). In addition to those data quality filters, a 'surface rejection' filter was applied as a percentage of the range to sea-surface (or sea-bottom for the downward looking F3B09&10) usually equal to 10% (i.e. a little higher than the theoretical 6% stated for 20° beam angle ADCPs, T-RDI documentation #P/N 951-6069-00 p38). Trial and error was performed for this latter filter by examining the velocity, backscatter and correlation profiles of each of the timeseries. In the case of severely tilted instrument (details below) up to 30% of the range needed to be removed. Speed, PG and surface rejection filters were applied to all the velocity and backscatter data while tilt filter was only applied to the current velocity direction and 'earth' components of the velocity data (i.e. eastward u, northward v and vertical w; details in technical validation section). For the other instruments, 'out-of-range' filters were based on the expected ranges, i.e. values that would be realistically impossible to attain within the study area, and/or based on default values given automatically to bad data by the logger (e.g. PAR and Qs < 0, see Table 2 for details).

6) a manual 'despiking' was finally performed by plotting the data and examining the timeseries visually. Minimal rejection was done to avoid rejecting potential 'outlier events'. As a result, some spurious data points may still be present in some timeseries.

The CTD profiles were processed using SBE data analysis software and recommended procedure as described in Donnet et al. (2018a). CTD profiles were averaged in 1 m bins and visually checked individually.

Table 2: 'out-of-range' filters used to quality control the data.

Instrument	Criteria
ADCP	Speed<0 m/s
	PG<25%
	Tilt>15º
	Surface rejection (8-30% range)
CTD	Depth < 0.5 m or > 250 m
	Temperature < -2ºC or > 25ºC
	Salinity < 5 or > 37
UTBI	Temperature < -2ºC or > 25ºC
U20	Depth < 0.5 m or > 250 m
	Temperature < -2ºC or > 25ºC
Mastodon	Temperature < -2ºC or > 25ºC
Weather stations	Wind speed < 0.05 or > 40 m/s
	Atmospheric pressure < 850 or > 1069 mbar
	Temperature < -60ºC or > 60ºC
	PAR < 0 umol/m^2/s
	Qs < 0 W/m^2
Tide gauge	Depth < 0.5 m or > 5 m
	Temperature < -2ºC or > 25ºC

4.4 UTBI depth calculation

Since our thermistors (UTBI) did not have embedded pressure sensors, the depth of their temperature records needed to be estimated. This calculation was done in three steps, increasing the accuracy of the estimate at each step:

1) Once a site depth was accurately determined, mean depth of each UTBI was determined using the mooring diagrams providing with the distance from sea-bottom of each instrument. Mean depth (with respect to Mean Sea Level, MSL) was then determined as: site depth – height above sea bottom.

2) 'tidal depth', i.e. depth varying due to the tide alone, was determined using the results of tidal analyses made on the instruments equipped with a pressure sensor (i.e. ADCP, CTD and U20). One reference per mooring line was used, typically the instrument located the closest to the top of the mooring having the highest data coverage so that

the overall mooring tilt was best approximated (CTD or U20). Tidal analysis was done using the T_TIDE programs (Pawlowicz et al., 2002) and UTBI 'tidal depth' were calculated as: MSL depth + tide.

3) Finally, to take the mooring movement into account, i.e. lateral movements of the mooring line due to currents drag, an 'absolute depth' was determined using an estimate of the mooring horizontal tilt angle. Tilt angle was determined using the same depth timeseries from which a tidal analysis was performed for the previous step. A water level residual was then calculated as: measured water level (from MSL) – tide. This residual was then used to calculate a mooring line tilt angle series as: tilt = acos(H/L) where H is the instrument height above sea-bottom at any given time and L is the instrument height at rest (i.e. its mean height). Using the horizontal tilt angle timeseries, UTBI series of height above sea-bottom were calculated as: H = L x cos(tilt) where L is the UTBI height above sea-bottom at rest. The 'absolute depth' series was then determined as: site depth - H + tide.

Overall, the mooring lines average vertical tilt were below 5° (2-4° with a standard deviation of order 1-2°) with maximums on order 15-25° during extreme events, corresponding to mooring vertical displacements of about 5-15 m. These vertical 'knock-down' are large compared to the 1-2 m tidal range reported in the region (Donnet et al., 2018b) but relatively small in comparison to the mooring line length (about 5-10%), indicating good mooring performances.

It should be noted that these estimates of tilt and therefore instrument depths assume no other external variation of sea-level than the tides. Other factors such as storm surges or shelf waves can affect the sea-level on the order of 0.2-1 m in the region (e.g. Tang et al., 1998, Thiebaut and Vennel, 2010, Han et al., 2012 and Ma et al., 2015). A preliminary inspection of our tide gauge records (not shown) indicate that residuals, i.e. water level variations not attributed to tides, of the same range was observed during our program.

4.5 In-situ comparisons (e.g. CTD profile vs. mooring data)

A CTD cast was performed after each mooring deployment and just before mooring recovery (see Figure 6 as example). Thus, a total of 52 casts were available for in-situ checks (F3B03 and F3B04 pre-recovery casts were missed). The primary goal of those checks were to assess the performance of the moored UTBI lines (Temperature) and moored CTDs (Salinity).

Overall, a mean difference of 0.12°C and associated mean standard deviation of 0.11°C was found between the CTD profiles and UBTI observations and an overall mean salinity difference of 0.07 and mean standard deviation of 0.03 between the CTD profiles and moored CTD was obtained.

F3B01 201611 post-dpt, cast#61067038 SBE19#6523
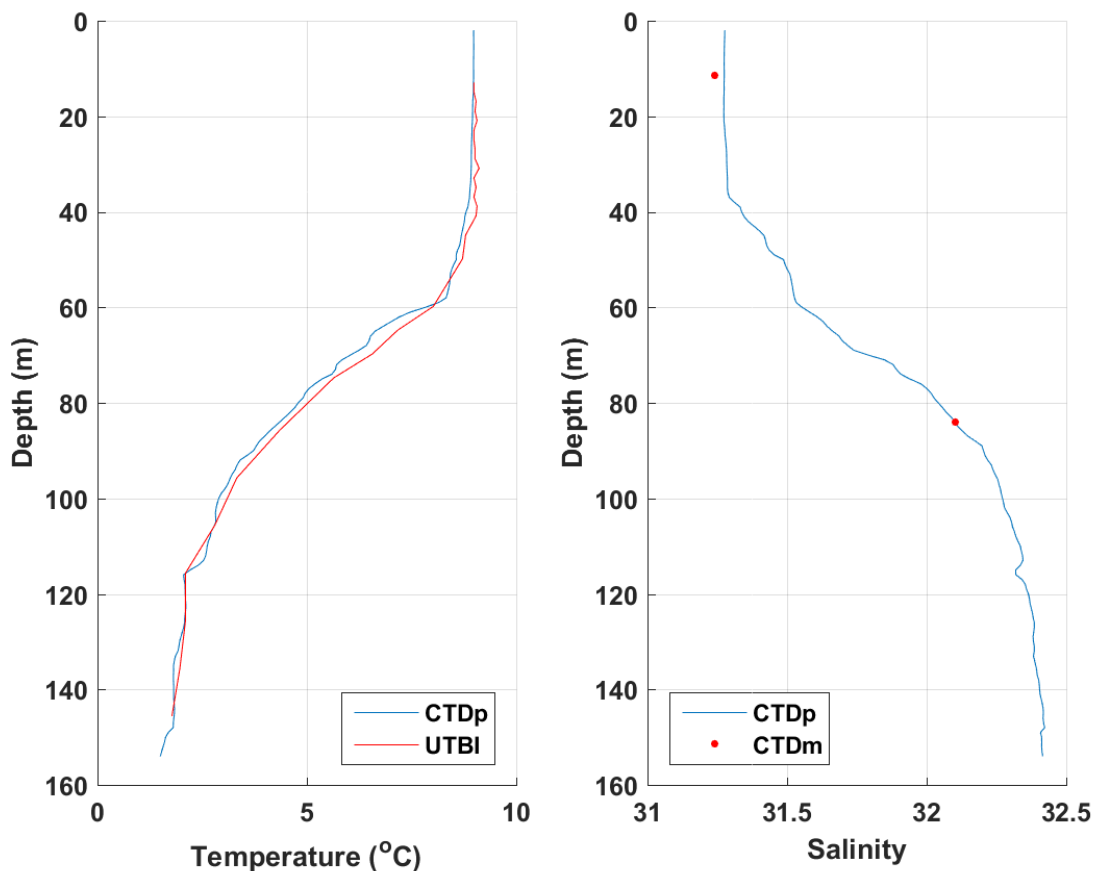
Figure 6: in-situ CTD profile (CTDp) comparison with moored thermistors (UTBI) and moored CTD (CTDm) on November 07, 2016 at F3B01

4.6 ADCP tilt issue

Excessive vertical tilt affects ADCPs' gyrocompass by biasing the heading which corrupt trigonometric rotation from instrument coordinates to earth coordinates (T-RDI pers. Com. and details in T-RDI documentation #P/N 951-6079-00). T-RDI indicates that while their attitude sensor can measure tilts (i.e. pitch and roll) up to about 20°, tilts above 15° will irreversibly corrupt the data (T-RDI documentation #P/N 957-6150-00, p17). If the tilt, however, stays within measurable range (i.e. 15° to about 20°) bin mapping will still hold (T-RDI pers. Com.; see details in T-RDI documentation #P/N 951-6079-00) and, thus, horizontal measurements of current speed and backscatter, i.e. variables not affected by erroneous heading, will still be correct and properly 'mapped'. At 20°, any given beam may end-up being oriented horizontally which prevents from deriving the horizontal component of the current; 3 beam solution may still work but the flow horizontal homogeneity assumption cannot be assessed (the so called 'error velocity', see T-RDI documentation #P/N 951-6069-00 p14 and P/N 957-6150-00, p14 for details) thereby limiting quality control. Beyond the tilt sensor limits (i.e. in pitch and roll axes) which can

be anywhere from 20 to about 25 degree (see Table 3), current speed calculation and bin mapping will become biased; profiles data will then likely be unrecoverable. An illustration of this issue and potential recoverable data is presented in Figure 7. Top 50 m (not affected by over-tilted position) and bottom (over tilted from December 7th) ADCP profiles are plotted together, showing the effects of the tilt on current direction and current vertical component w but not on current speed and acoustic backscatter.

In our quality control process, a 'combined' tilt angle, i.e. combination of pitch and roll angles, were used to filter unreliable current direction and earth coordinates velocities (i.e. u, v and w). This 'combined' tilt was calculated as follow:

$$tilt = acos(cos(pitch).*cos(roll))$$

This rejection is somehow conservative since this 'combined' angle is always larger than the pitch and roll taken individually. In addition to this automatic filter, bench tests were performed on each of our ADCPs to determine their maximum pitch and roll angles measurable by placing each unit horizontally on a table on each direction, i.e. Beam 1-2 and Beam 3-4 axes which helped us to further assess the quality of our data (Table 3).

Five timeseries were affected by this issue in total: F3B01 leg 2 (bottom unit), F3B01 leg 3, F3B05 leg 3&4 and F3B07 leg 3. Being tilted near both pitch and roll limits, the latter was corrupted beyond repair and nothing could be saved from it. The other four were generally severely tilted, but below the limits and on one side 'only'; current speed and backscatter profiles were saved from those timeseries.

Table 3: Severely tilted timeseries screening

Site and leg	Mean Pitch (°)	Mean Roll (°)	Max Pitch (°) (bench)	Max Roll (°) (bench)
F3B01, leg 2	18.1	-0.3	24.2	23.5
F3B01, leg 3	-10.1	25.9	24.8	26.4
F3B05, leg 3	22.0	-1.1	24.2	23.5
F3B07, leg 3	24.2	23.4	24.8	24.7
F3B05, leg 4	21.5	-0.3	24.2	23.5
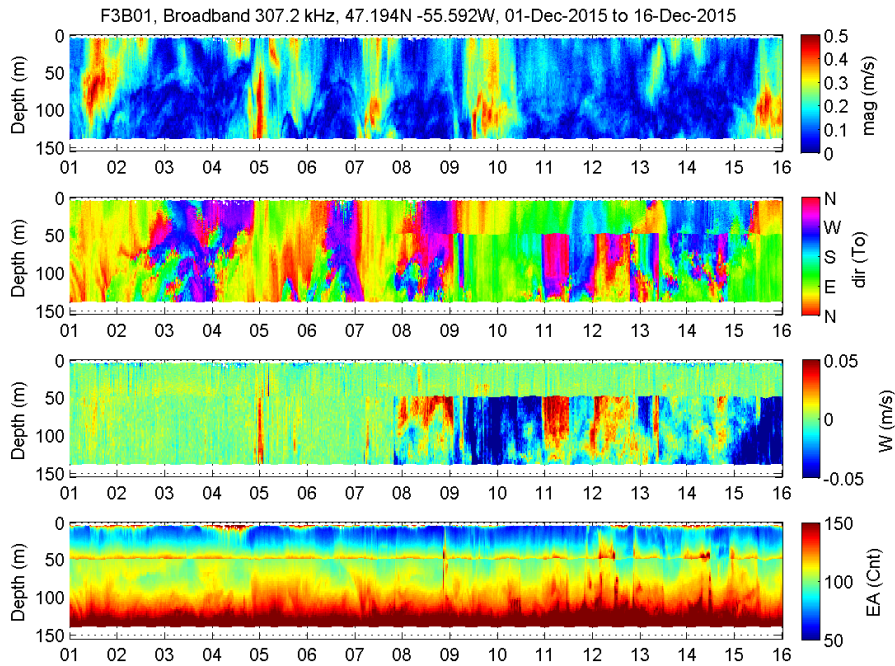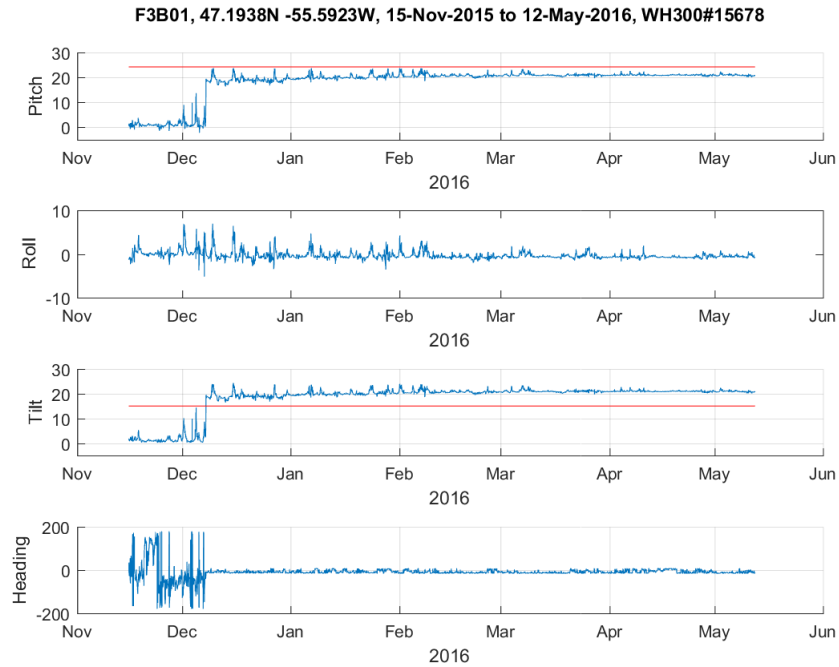
Figure 7: Example of an ADCP over-tilted issue. The event occurred on December 7, 2015 between 18:30 and 19:30, tilting the
385 **bottom ADCP of the mooring line on the pitch axis. Top four panels show the attitude sensor, pitch (1st panel), roll (2nd panel), calculated 'combined' tilt angle (3rd panel) and heading (4th panel and as recorded by the instrument). Red lines on the pitch and tilt plots indicate the maximum sensor range as determined by bench test and the maximum accepted tilt angle of our quality control filter, respectively. The bottom four panels show current speed (mag), current direction (dir), current vertical component (w) and raw backscatter data (EA) zooming on the period 1-16 December 2015.**

5 Data availability

Processed data are available from the SEANOE repository (https://doi.org/10.17882/62314; Donnet and Lazure, 2020). One file per timeseries was created in the NetCDF format containing an header with key metadata (site ID, geographic coordinates, site depth, instrument used, author and date of creation) and the data themselves with consistent variable's naming (e.g. time, depth, temperature etc.). UTBI timeseries were bundled together into one folder per mooring line and, thus, 1 processed file per timeseries. CTD profiles were bundle-up per surveys and formatted as tab-delimited ASCII ODV4 files (Schlitzer, 2019). NetCDF files were created under the MATLAB environment and tested using the NetCDF utilities (ncdump from unidata), python (with xarray and panda libraries) and the Interactive Data Language (IDL) environments. Care was taken to export as much data from the raw as possible (e.g. ADCP correlation magnitudes) but are provided as 'processed', that is, bad data flagged by the QA/QC (Quality Assessment/Quality Control) process described below were replaced by NaN (Not a Number) values.

6 Conclusion

We present an oceanographic dataset collected in a subpolar, mid-latitude, broad fjord. The data collection was centered on the deployment and recovery of oceanographic moorings and a few land-based stations collecting physical parameters such as: water temperature and salinity, ocean currents, wind speed and direction and tide. The main goal of this observation program was to serve as a base to further study the main physical processes affecting this embayment which are likely common to other wide stratified fjords.

To our knowledge, very few embayments alike, i.e. broad fjords, have such comprehensive observations combining numerous and continuous in-situ sampling points. Several bays in the region have been well explored in the past but their continuous observation via moorings rarely extended more than a few months during the spring to fall seasons, thus not offering a complete seasonal picture (e.g. Yao 1986, de Young and Sanderson 1995, Hart et al. 1999, Schillinger et al. 2000, Tittensor et al. 2002a&b). Abroad, with the increasing interest in polar regions and their importance in climate, many recent studies relied on significant datasets collected in broad fjords (e.g. Straneo et al. 2010, Jackson et al. 2014, Inall et al. 2015, Merrifield et al. 2018). Generally, and most likely due to extremely challenging technical constraints (e.g. massive glacial ice), those datasets remain scarce and limited to a few points and/or few months observation, however. A notable exception to this scarcity is the important research effort spent in the Svalbard since 2002 (see Hop et al. 2019 for a review).

By combining a relatively large number of observation points (up to 21 moorings during leg 3), high vertical resolution in both thermal stratification (2-10 m) and ocean currents (1-3 m) as well as duration (2-years), we believe that this dataset should be comprehensive enough to study a wide variety of processes; making it of particular interest to be shared.

Authors contribution

420   SD designed the study with the assistance of PL, AWR and GH. SD designed and directed the fieldwork, including the moorings design and pre-implementation modelling. SD processed all the data except those from the Mastodon, which were processed by PL. SD, designed and led the QA/QC procedures and data analyses with contributions from PL, AWR and GH. SD prepared the figures and wrote the manuscript with contributing reviews from PL, AWR and GH.

Competing interests

425   The authors declare that they have no conflict of interest.

Disclaimer

Data are published without any warranty, express or implied. The user assumes all risks arising from his/her use of data. Data are intended to be research-quality. It is the sole responsibility of the user to assess if the data are appropriate for his/her use, and to interpret the data, data quality, and data accuracy accordingly. Authors welcome users to ask questions and report

430   problems.

Acknowledgements

A number of people contributed to the field effort and to which we are very grateful; many thanks to: Dwight Drover (DFO leg 2-4), Pierre Goulet (DFO leg 1&2), Kim Marshall (DFO leg 2), Sharon Kenny (DFO leg 2), Shannon Cross (DFO leg 3), Marion Bezaud (DFO-IFREMER leg 4), Herle Goraguer (IFREMER) and Jean-Pierre Claireaux (DTAM; IFREMER data).

435   This program was funded by DFO's ACRDP (Aquaculture Collaborative Research and Development Program) in partnership with Cold Ocean Salmon (COS), Northern Harvest Sea Farms Ltd. and Newfoundland Aquaculture Industry Association (NAIA). IFREMER's contribution was funded by DTAM (Direction des Territoires de l'Alimentation et de la Mer, Saint-Pierre et Miquelon). We also thank Shannon Cross and Daria Gallardi for their kind assistance in preparing Figure 1 and Figure 2 (respectively). Finally, we wish to thank the reviewers for their constructive remarks; helping to improve the manuscript.

440   **References**

Cottier, F. R., Nilsen, F., Skogseth, R., Tverberg, V., Skardhamar, J. and Svendsen, H.: Arctic fjords: a review of the oceanographic environment and dominant physical processes, in Fjord Systems and Archives, vol. 344, edited by M. (eds) Howe J. A. ,. Austin, W. E. N. ,. Forwick, M. &. Paetzel, pp. 35–50, Geological Society, London, 2010.

445 Cushman-Roisin, B., Asplin, L. and Svendsen, H.: Upwelling in broad fjords, Continental Shelf Research, 14, 1701–172, 1994.

Davidson, F. J. M., Greatbatch, R. J. and de Young, B.: Asymmetry in the response of a stratified coastal embayment to wind forcing, Journal of Geophysical Research, 106, 7001–7015, 2001.

Deines, K. L.: Backscatter Estimation Using Broadband Acoustic Doppler Current Profilers, in Proceedings of the IEEE Sixth

450 Working Conference on Current Measurement, pp. 249–253, IEEE, San Diego (CA)., 1999.

de Young, B. and Hay, A. E.: Density current flow into Fortune Bay, Newfoundland, Journal of Physical Oceanography, 17, 1066–1070, 1987.

455 de Young, B. and Sanderson, B.: The circulation and hydrography of conception bay, Newfoundland, Atmosphere-Ocean, 33, 135–162, 1995.

de Young, B., Otterson, T. and Greatbatch, R. J.: The Local and Nonlocal Response of Conception Bay to Wind Forcing, Journal of Physical Oceanography, 23, 2636–2649, 1993.

460

de Young, B. S.: Deep water exchange in Fortune Bay, Newfoundland, Memorial University of Newfoundland, St John's., 1983.

Donnet, S., Lazure, P.: Fortune Bay (NL, Canada) oceanographic observations May 2015 - May 2017. SEANOE.

465 https://doi.org/10.17882/62314, 2020

Donnet, S., Cross, S., Goulet, P. and Ratsimandresy, A. W.: Coast of Bays seawater vertical and horizontal structure (2009-13): Hydrographic structure, spatial variability and seasonality based on the Program for Aquaculture Regulatory Research (PARR) 2009-13 oceanographic surveys, Fisheries and Oceans, Canadian Science Advisory Secretariat, Ottawa, ON., 2018a.

470

Donnet, S., Ratsimandresy, A. W., Goulet, P., Doody, C., Burke, S. and Cross, S.: Coast of Bays metrics: Geography, Hydrology and Physical Oceanography of an aquaculture area of the South Coast of Newfoundland, Fisheries and Oceans, Canadian Science Advisory Secretariat, Ottawa, ON., 2018b.

475 Dunbar, M. J.: Eastern Arctic Waters, Fisheries Research Board of Canada, Ottawa, 1951.

Dunbar, M. J.: Arctic and Subarctic Marine Ecology: Immediate Problems, Arctic, 7, 213–228, 1953.

Farmer, D. M. and Freeland, H. J.: The Physical Oceanography of Fjords, Progress in Oceanography, 12, 147–194, 1983.

480

Hamilton, J. M., Fowler, G. A. and Belliveau, D. J.: Mooring Vibration as a Source of Current Meter Error and Its Correction, Journal of Atmospheric and Oceanic Technology, 14, 644–655, 1997.

Han, G., Ma, Z., Chen, D., de Young, B. and Chen, N.: Observing storm surges from space: Hurricane Igor off Newfoundland, 485 Nature: Scientific Reports, 2, 1–9, 2012.

Hart, D. J., de Young, B. and Foley, J.: Observations of Currents, Temperature and Salinity in Placentia Bay, Newfoundland 1998-9, Memorial University of Newfoundland, St John's (NL)., 1999.

490 Hay, A. E. and de Young, B.: An Oceanographic Flip-Flop: Deep Water Exchange in Fortune Bay, Newfoundland, Journal of Geophysical Research, 94, 843–853, 1989.

Hop, H., Cottier, F. and Berge, J.: Autonomous Marine Observatories in Kongsfjorden, Svalbard, in The Ecosystem of Kongsfjorden, Svalbards, Advances in Polar Ecology 2, edited by Hop H. and Wiencke C., pp. 515-533, Springer Nature 495 Switzerland, 2019.

Inall, M. E. and Gillibrand, P. A.: The physics of mid-latitude fjords: a review, in Fjord Systems and Archives, vol. 344, edited by M. (eds) Howe J. A. ,. Austin, W. E. N. ,. Forwick, M. &. Paetzel, pp. 17–33, Geological Society, London, 2010.

500 Inall, M. E., Nilsen, F., Cottier, F. R. and Daae, R.: Shelf/fjord exchange driven by coastal-trapped waves, Journal of Geophysical Research: Oceans, 120, 8283–8303, 2015.

Jackson, R. H., Straneo, F. and Sutherland, D. A.: Externally forced fluctuations in ocean temperature at Greenland glaciers in non-summer months, Nature Geoscience, 7, 503, 2014.

505

Jackson, R. H., Lentz, S. J. and Straneo, F.: The Dynamics of Shelf Forcing in Greenlandic Fjords, Journal of Physical Oceanography, 48, 2799–2827, 2018.

Lazure, P., Le Cann, B. and Bezaud, M.: Large diurnal bottom temperature oscillations around the Saint Pierre and Miquelon 510 archipelago, Scientific Reports, 8, 13882, 2018.

Ma, Z., Han, G. and de Young, B.: Modelling Temperature, Currents and Stratification in Placentia Bay, Atmosphere-Ocean, 50, 244–260, 2012.

515 Ma, Z., Han, G. and de Young, B.: Oceanic responses to Hurricane Igor over the Grand Banks: A modeling study, Journal of Geophysical Research: Oceans, 120, 1276–1295, 2015.

Merrifield, S., Otero, M. and Terrill, E.: Observations of Shelf Exchange and High-Frequency Variability in an Alaskan Fjord, Journal of Geophysical Research: Oceans, 123, 4720–4734, 2018.
520
Mullison, J.: Backscatter Estimation Using Broadband Acoustic Doppler Current Profilers-Updated, ASCE, Durham., 2017.

Pawlowicz, R., Beardsley, B. and Lentz, S.: Classical tidal harmonic analysis including error estimates in MATLAB using T_TIDE, Computers & Geosciences, 28, 929–937, 2002.
525
Ratsimandresy, A. W., Donnet, S., Goulet, P., Bachmayer, R. and Claus, B.: Variation in the structure of the water column as captured by Slocum glider CTD and by CTD from a research vessel and assessment of internal waves, pp. 1–10, IEEE, St. John's, NL., 2014.

530 Ratsimandresy, A. W., Donnet, S., Snook, S. and Goulet, P.: Analysis of the variability of the ocean currents in the Coast of Bays area, Fisheries and Oceans, Canadian Science Advisory Secretariat, Ottawa, ON., 2019.

Richard, J. M.: The mesopelagic fish and invertebrate macrozooplankton faunas of two Newfoundland fjords with differing physical oceanography, Memorial University of Newfoundland, St John's., 1987.
535
Richard, J. M. and Haedrich, R. L.: A comparison of the macrozooplankton faunas in two newfoundland fjords differing in physical oceanography, Sarsia, 76, 41–52, 1991.

Salcedo-Castro, J. and Ratsimandresy, A. W.: Oceanographic response to the passage of hurricanes in Belle Bay, 540 Newfoundland, Estuarine, Coastal and Shelf Science, 133, 224–234, 2013.

Schillinger, D., Simmons, P. and de Young, B.: Analysis of the Mean Circulation in Placentia Bay: Spring and Summer 1999, Memorial University of Newfoundland, St John's (NL)., 2000.

545   Stigebrandt, A.: Hydrodynamics and Circulation of Fjords, in Encyclopedia of Lakes and Reservoirs, vol. Encyclopedia of Earth Sciences Series, edited by F. R. W. (eds) Bengtsson L. Herschy R. W., pp. 327–344, Springer, Dordrecht., 2012.

Straneo, F. and Cenedese, C.: The Dynamics of Greenland's Glacial Fjords and Their Role in Climate, Annual Review of Marine Science, 7, 89–112, 2015.

550

Straneo, F., Hamilton, G. S., Sutherland, D. A., Stearns, L. A., Davidson, F., Hammill, M. O., Stenson, G. B. and Rosing-Asvid, A.: Rapid circulation of warm subtropical waters in a major glacial fjord in East Greenland, Nature Geoscience, 3, 182, 2010.

555   Tang, C. L., Gui, Q. and DeTracey, B. M.: Barotropic Response of the Labrador/Newfoundland Shelf to a Moving Storm, Journal of Physical Oceanography, 28, 1152–1172, 1998.

Thiebaut, S. and Vennell, R.: Observation of a Fast Continental Shelf Wave Generated by a Storm Impacting Newfoundland Using Wavelet and Cross-Wavelet Analyses, Journal of Physical Oceanography, 40, 417–428, 2010.

560

Tittensor, D. P., Naud, R., de Young, B. and Foley, J.: Analysis of Physical Oceanographic Data from Trinity Bay, May – August 2001, Memorial University of Newfoundland, St John's (NL)., 2002a.

Tittensor, D. P., de Young, B. and Foley, J.: Analysis of Physical Oceanographic Data from Trinity Bay, May – August 2002, 565   Memorial University of Newfoundland, St John's (NL)., 2002b.

White, M. and Hay, A. E.: Dense overflow into a large silled embayement: Tidal modulation, fronts and basin modes, Journal of Marine Research, 52, 459–487, 1994.

570   Yao, T.: The Response of Currents in Trinity Bay, Newfoundland, to Local Wind Forcing, Atmosphere-Ocean, 24, 235–252, 1986.

Appendix A

575   **Figure A-1: Pool's Cove (POOLC) tide gauge (left) and Dog Island (DOGIS) weather stations (right)**

Appendix B

Table B-1: Data collection summary, Leg 1 (May 2015 – November 2015)

Site	Instrument	Latitude (ºN)	Longitude (ºW)	Deployment	Recovery	Site Depth	Instrument Depth	% Coverage
F3B01	WH300#12548	47.193717	-55.590867	2015-05-04T12:53:40	2015-11-14T15:33:00	151	51	97
F3B01	WH300#15678	47.193717	-55.590867	2015-05-04T12:53:40	2015-11-14T15:33:00	151	142	88
F3B01	RBR#60134	47.194990	-55.588950	2015-05-04T16:24:10	2015-11-14T15:47:00	151	2	75
F3B01	SBE19#1019	47.194990	-55.588950	2015-05-04T16:24:10	2015-11-14T15:47:00	151	81	77
F3B01	U20#10305634	47.194990	-55.588950	2015-05-04T16:24:10	2015-11-14T15:47:00	151	20	100
F3B01	UTBIs	47.193717	-55.590867	2015-05-04T12:53:40	2015-11-14T15:33:00	151	62-132	100
F3B01	UTBIs	47.194990	-55.588950	2015-05-04T16:24:10	2015-11-14T15:47:00	151	20-141	95
F3B02	WH300#15677	47.342718	-55.717833	2015-05-04T22:29:35	2015-11-14T13:07:00	153	53	98
F3B02	WH300#19001	47.342718	-55.717833	2015-05-04T22:29:35	2015-11-14T13:07:00	153	142	86
F3B02	SBE19#1318	47.339410	-55.923850	2015-05-04T19:51:20	2015-11-14T13:42:00	152	82	100
F3B02	U20#10214891	47.339410	-55.923850	2015-05-04T19:51:20	2015-11-14T13:42:00	152	21	100
F3B02	UTBIs	47.342718	-55.717833	2015-05-04T22:29:35	2015-11-14T13:07:00	153	64-134	100
F3B02	UTBIs	47.33941	-55.923850	2015-05-04T19:51:20	2015-11-14T13:42:00	152	21-142	91
F3B03	WH300#13951	47.557343	-55.332225	2015-05-05T13:22:01	2015-11-17T15:17:00	157	57	97
F3B03	WH300#13772	47.557343	-55.332225	2015-05-05T13:22:01	2015-11-17T15:17:00	157	148	86
F3B03	SBE37#10571	47.557470	-55.329050	2015-05-05T15:09:07	2015-11-16T11:57:00	154	10	100
F3B03	SBE19#2245	47.557470	-55.329050	2015-05-05T15:09:07	2015-11-16T11:57:00	154	81	100
F3B03	UTBIs	47.557343	-55.332225	2015-05-05T13:22:01	2015-11-17T15:17:00	157	68-138	100
F3B03	UTBIs	47.557470	-55.329050	2015-05-05T15:09:07	2015-11-16T11:57:00	154	11-142	96
F3B04	WH300#17956	47.635950	-55.281008	2015-05-08T12:56:00	2015-11-16T14:39:00	146	46	98
F3B04	WH300#11351	47.635950	-55.281008	2015-05-08T12:56:00	2015-11-16T14:39:00	146	137	91
F3B04	SBE37#10572	47.632540	-55.277480	2015-05-08T11:46:00	2015-11-16T14:54:00	260	6	100
F3B04	SBE19#2246	47.632540	-55.277480	2015-05-08T11:46:00	2015-11-16T14:54:00	260	78	100
F3B04	UTBIs	47.635950	-55.281008	2015-05-08T12:56:00	2015-11-16T14:39:00	146	57-127	100
F3B04	UTBIs	47.632540	-55.277480	2015-05-08T11:46:00	2015-11-16T14:54:00	260	7-139	100

580

Table B-2: Data collection summary, Leg 2 (November 2015 – May 2016)

Site	Instrument	Latitude (ºN)	Longitude (ºW)	Deployment	Recovery	Site Depth	Instrument Depth	% Coverage
F3B01	WH300#12548	47.193783	-55.592287	2015-11-15T15:47:00	2016-05-12T17:05:00	152	52	98
F3B01	WH300#15678	47.193783	-55.592287	2015-11-15T15:47:00	2016-05-12T17:05:00	152	143	51
F3B01	RBR#22032	47.196250	-55.587187	2015-11-15T16:00:00	2016-05-10T16:35:00	152	11	100
F3B01	SBE19#1319	47.196250	-55.587187	2015-11-15T16:00:00	2016-05-10T16:35:00	152	11	100
F3B01	SBE19#1309	47.196250	-55.587187	2015-11-15T16:00:00	2016-05-10T16:35:00	152	82	100
F3B01	U20#10305634	47.196250	-55.587187	2015-11-15T16:00:00	2016-05-10T16:35:00	152	21	100
F3B01	UTBIs	47.193783	-55.592287	2015-11-15T15:47:00	2016-05-12T17:05:00	152	63-133	100
F3B01	UTBIs	47.196250	-55.587187	2015-11-15T16:00:00	2016-05-10T16:35:00	152	11-142	96
F3B02	WH300#15677	47.342547	-55.717868	2015-11-15T13:34:00	2016-05-10T12:35:00	153	53	98
F3B02	WH300#19001	47.342547	-55.717868	2015-11-15T13:34:00	2016-05-10T12:35:00	153	144	89
F3B02	RBR#22031	47.339265	-55.717860	2015-11-15T12:52:00	2016-05-11T19:00:00	152	11	100
F3B02	SBE19#1317	47.339265	-55.717860	2015-11-15T12:52:00	2016-05-11T19:00:00	152	11	100
F3B02	SBE19#1313	47.339265	-55.717860	2015-11-15T12:52:00	2016-05-11T19:00:00	152	82	100
F3B02	U20#10305633	47.339265	-55.717860	2015-11-15T12:52:00	2016-05-11T19:00:00	152	19	100
F3B02	U20#10214891	47.339265	-55.717860	2015-11-15T12:52:00	2016-05-11T19:00:00	152	21	100
F3B02	UTBIs	47.342547	-55.717868	2015-11-15T13:34:00	2016-05-10T12:35:00	153	64-134	100
F3B02	UTBIs	47.339265	-55.717860	2015-11-15T12:52:00	2016-05-11T19:00:00	152	11-142	100
F3B03	WH300#13951	47.557268	-55.331988	2015-11-17T18:06:00	2016-05-13T15:30:00	152	52	98
F3B03	WH300#13772	47.557268	-55.331988	2015-11-17T18:06:00	2016-05-13T15:30:00	152	143	84
F3B03	SBE37#10571	47.558150	-55.328900	2015-11-17T18:34:00	2016-05-13T15:58:00	160	16	100
F3B03	SBE19#1312	47.558150	-55.328900	2015-11-17T18:34:00	2016-05-13T15:58:00	160	88	33
F3B03	UTBIs	47.557268	-55.331988	2015-11-17T18:06:00	2016-05-13T15:30:00	152	63-133	100
F3B03	UTBIs	47.558150	-55.328900	2015-11-17T18:34:00	2016-05-13T15:58:00	160	17-148	100
F3B04	WH300#11351	47.635963	-55.281208	2015-11-17T11:26:00	2016-05-13T17:40:00	146	137	82
F3B04	WH300#17956	47.635963	-55.281208	2015-11-17T11:26:00	2016-05-13T17:40:00	146	46	99
F3B04	SBE37#10572	47.632508	-55.277488	2015-11-17T12:05:00	2016-05-13T17:55:00	260	5	100
F3B04	UTBIs	47.635963	-55.281208	2015-11-17T11:26:00	2016-05-13T17:40:00	146	57-127	100
F3B04	UTBIs	47.632508	-55.277488	2015-11-17T12:05:00	2016-05-13T17:55:00	260	7-138	100

585

Table B-3: Data collection summary, Leg 3 (May 2016 –November 2016)

Site	Instrument	Latitude (ºN)	Longitude (ºW)	Deployment	Recovery	Site Depth	Instrument Depth	% Coverage
F3B01	WH300#12548	47.193460	-55.592130	2016-05-13T11:11:00	2016-10-31T18:30:00	150	76	36
F3B01	RBR#22031	47.193460	-55.592130	2016-05-13T11:11:00	2016-10-31T18:30:00	150	6	100
F3B01	SBE19#1317	47.193460	-55.592130	2016-05-13T11:11:00	2016-10-31T18:30:00	150	6	82
F3B01	SBE19#1313	47.193460	-55.592130	2016-05-13T11:11:00	2016-10-31T18:30:00	150	78	100
F3B01	U20#10305633	47.193460	-55.592130	2016-05-13T11:11:00	2016-10-31T18:30:00	150	14	100
F3B01	U20#10214891	47.193460	-55.592130	2016-05-13T11:11:00	2016-10-31T18:30:00	150	16	100
F3B01	UTBIs	47.193460	-55.592130	2016-05-13T11:11:00	2016-10-31T18:30:00	150	6-139	100
F3B02	WH300#15677	47.331913	-55.737182	2016-05-11T16:05:00	2016-10-31T16:52:00	153	79	98
F3B02	RBR#22032	47.331910	-55.737180	2016-05-11T16:05:00	2016-10-31T16:52:00	153	9	100
F3B02	SBE19#1319	47.331910	-55.737180	2016-05-11T16:05:00	2016-10-31T16:52:00	153	9	65
F3B02	SBE19#1309	47.331910	-55.737180	2016-05-11T16:05:00	2016-10-31T16:52:00	153	81	100
F3B02	U20#10305636	47.331910	-55.737180	2016-05-11T16:05:00	2016-10-31T16:52:00	153	17	100
F3B02	U20#10305634	47.331910	-55.737180	2016-05-11T16:05:00	2016-10-31T16:52:00	153	19	100
F3B02	UTBIs	47.331910	-55.737180	2016-05-11T16:05:00	2016-10-31T16:52:00	153	9-142	97
F3B03	WH300#13951	47.524650	-55.340300	2016-05-16T17:00:00	2016-11-02T18:05:00	161	87	97
F3B03	SBE37#10571	47.524650	-55.340330	2016-05-16T17:00:00	2016-11-02T18:05:00	161	16	100
F3B03	RBR#60334	47.524650	-55.340330	2016-05-16T17:00:00	2016-11-02T18:05:00	161	87	100
F3B03	UTBIs	47.524650	-55.340330	2016-05-16T17:00:00	2016-11-02T18:05:00	161	17-149	100
F3B04	WH300#11348	47.639650	-55.297100	2016-05-16T15:00:00	2016-11-04T16:15:00	163	79	98
F3B04	SBE37#10572	47.639650	-55.297130	2016-05-16T15:00:00	2016-11-04T16:15:00	163	8	100
F3B04	SBE19#1315	47.639650	-55.297130	2016-05-16T15:00:00	2016-11-04T16:15:00	163	80	100
F3B04	UTBIs	47.639650	-55.297130	2016-05-16T15:00:00	2016-11-04T16:15:00	163	9-141	100
F3B05	WH300#15678	47.303670	-55.355600	2016-05-13T12:55:00	2016-11-02T16:16:00	91	80	38
F3B05	SBE19#1316	47.303670	-55.355560	2016-05-13T12:55:00	2016-11-02T16:16:00	91	10	100
F3B05	SBE19#1019	47.303670	-55.355560	2016-05-13T12:55:00	2016-11-02T16:16:00	91	82	100
F3B05	UTBIs	47.303670	-55.355560	2016-05-13T12:55:00	2016-11-02T16:16:00	91	10-72	100
F3B06	WH300#19001	47.437130	-55.490800	2016-05-11T21:01:00	2016-11-02T14:50:00	89	78	98
F3B06	SBE19#1021	47.437130	-55.490810	2016-05-11T21:01:00	2016-11-02T14:50:00	89	8	100
F3B06	SBE19#1237	47.437130	-55.490810	2016-05-11T21:01:00	2016-11-02T14:50:00	89	80	100
F3B06	UTBIs	47.437130	-55.490810	2016-05-11T21:01:00	2016-11-02T14:50:00	89	8-70	100
F3B07	WH300#13772	47.601870	-55.386500	2016-05-15T18:20:00	2016-11-03T14:30:00	96	85	0
F3B07	SBE19#1483	47.601870	-55.386480	2016-05-15T18:20:00	2016-11-03T17:00:00	96	15	100
F3B07	SBE19#1312	47.601870	-55.386480	2016-05-15T18:20:00	2016-11-03T14:30:00	96	87	33
F3B07	UTBIs	47.601870	-55.386480	2016-05-15T18:20:00	2016-11-03T14:30:00	96	15-77	96

F3B08	WH300#17956	47.580850	-55.168450	2016-06-14T13:09:00	2016-11-05T16:24:00	209	90	98
F3B08	SBE19#1318	47.580833	-55.168433	2016-06-14T13:09:00	2016-11-05T16:24:00	209	19	100
F3B08	RBR#60335	47.580833	-55.168433	2016-06-14T13:09:00	2016-11-05T16:24:00	209	91	100
F3B08	UTBIs	47.580833	-55.168433	2016-06-14T13:09:00	2016-11-05T16:24:00	209	20-82	100
F3B09	WH600#12391	47.633100	-55.440300	2016-05-14T16:56:00	2016-11-03T17:47:00	58	6	48
F3B09	SBE37#14435	47.633100	-55.440280	2016-05-14T16:56:00	2016-11-03T17:47:00	58	7	100
F3B09	SBE37#14436	47.633100	-55.440280	2016-05-14T16:56:00	2016-11-03T17:47:00	58	53	100
F3B09	UTBIs	47.633100	-55.440280	2016-05-14T16:56:00	2016-11-03T17:47:00	58	8-43	100
F3B10	WH600#12390	47.704750	-55.384100	2016-05-14T17:39:00	2016-11-03T19:55:00	58	6	17
F3B10	SBE37#14434	47.704750	-55.384060	2016-05-14T17:39:00	2016-11-03T19:55:00	58	7	100
F3B10	SBE37#14433	47.704750	-55.384060	2016-05-14T17:39:00	2016-11-03T19:55:00	58	53	97
F3B10	UTBIs	47.704750	-55.384060	2016-05-14T17:39:00	2016-11-03T19:55:00	58	8-43	100

590 **Table B-4: Mooring data collection summary, Leg 4 (November 2016 – May 2017)**

Site	Instrument	Latitude (ºN)	Longitude (ºW)	Deployment	Recovery	Site Depth	Instrument Depth	% Coverage
F3B01	WH300#12548	47.194520	-55.596913	2016-11-02T11:24:00	2017-05-08T17:40:00	156	82	99
F3B01	RBR#22031	47.194520	-55.596913	2016-11-02T11:24:00	2017-05-08T17:40:00	156	12	95
F3B01	SBE19#1317	47.194520	-55.596913	2016-11-02T11:24:00	2017-05-08T17:40:00	156	12	100
F3B01	SBE19#1313	47.194520	-55.596913	2016-11-02T11:24:00	2017-05-08T17:40:00	156	84	100
F3B01	U20#10214891	47.194520	-55.596913	2016-11-02T11:24:00	2017-05-08T17:40:00	156	22	100
F3B01	U20#10305633	47.194520	-55.596913	2016-11-02T11:24:00	2017-05-08T17:40:00	156	20	100
F3B01	UTBIs	47.194520	-55.596913	2016-11-02T11:24:00	2017-05-08T17:40:00	156	12-145	100
F3B02	WH300#15677	47.330532	-55.735460	2016-11-02T12:46:00	2017-05-08T11:59:00	157	83	100
F3B02	RBR#22032	47.330532	-55.735460	2016-11-02T12:46:00	2017-05-08T11:59:00	157	13	95
F3B02	SBE19#1319	47.330532	-55.735460	2016-11-02T12:46:00	2017-05-08T11:59:00	157	13	100
F3B02	SBE19#1309	47.330532	-55.735460	2016-11-02T12:46:00	2017-05-08T11:59:00	157	85	100
F3B02	U20#10305634	47.330532	-55.735460	2016-11-02T12:46:00	2017-05-08T11:59:00	157	23	100
F3B02	U20#10305636	47.330532	-55.735460	2016-11-02T12:46:00	2017-05-08T11:59:00	157	21	100
F3B02	UTBIs	47.330532	-55.735460	2016-11-02T12:46:00	2017-05-08T11:59:00	157	13-146	97
F3B03	WH300#13951	47.523800	-55.340675	2016-11-03T13:38:00	2017-05-09T13:05:00	159	85	99
F3B03	SBE37#10571	47.523800	-55.340675	2016-11-03T13:38:00	2017-05-09T13:30:00	159	15	100
F3B03	RBR#60334	47.523800	-55.340675	2016-11-03T13:38:00	2017-05-09T13:30:00	159	86	100
F3B03	UTBIs	47.523800	-55.340675	2016-11-03T13:38:00	2017-05-09T13:30:00	159	15-147	100
F3B04	WH300#11348	47.639702	-55.297115	2016-11-05T14:55:00	2017-05-10T11:07:00	160	76	100
F3B04	SBE37#10572	47.639702	-55.297115	2016-11-05T14:55:00	2017-05-10T11:07:00	160	5	100
F3B04	SBE19#1315	47.639702	-55.297115	2016-11-05T14:55:00	2017-05-10T11:07:00	160	77	100

F3B04	UTBIs	47.639702	-55.297115	2016-11-05T14:55:00	2017-05-10T11:07:00	160	6-138	100
F3B05	WH300#15678	47.303605	-55.357987	2016-11-03T11:54:00	2017-05-08T15:36:00	96	85	39
F3B05	SBE19#1316	47.303605	-55.357987	2016-11-03T11:54:00	2017-05-08T15:36:00	96	15	100
F3B05	SBE19#1019	47.303605	-55.357987	2016-11-03T11:54:00	2017-05-08T15:36:00	96	87	100
F3B05	UTBIs	47.303605	-55.357987	2016-11-03T11:54:00	2017-05-08T15:36:00	96	15-77	100
F3B06	WH300#19001	47.434265	-55.490907	2016-11-03T11:20:00	2017-05-08T13:58:00	96	85	99
F3B06	SBE19#1021	47.434265	-55.490907	2016-11-03T11:20:00	2017-05-08T13:58:00	96	15	100
F3B06	SBE19#1237	47.434265	-55.490907	2016-11-03T11:20:00	2017-05-08T13:58:00	96	87	100
F3B06	UTBIs	47.434265	-55.490907	2016-11-03T11:20:00	2017-05-08T13:58:00	96	15-77	100
F3B07	WH300#13772	47.602237	-55.386593	2016-11-04T15:05:00	2017-05-10T12:26:00	104	93	95
F3B07	SBE19#1483	47.602237	-55.386593	2016-11-04T15:05:00	2017-05-10T12:26:00	104	23	99
F3B07	SBE19#1312	47.602237	-55.386593	2016-11-04T15:05:00	2017-05-10T12:26:00	104	95	33
F3B07	UTBIs	47.602237	-55.386593	2016-11-04T15:05:00	2017-05-10T12:26:00	104	23-85	100
F3B08	WH300#17956	47.579797	-55.168053	2016-11-06T15:00:00	2017-05-09T16:30:00	206	87	100
F3B08	SBE19#1318	47.579797	-55.168053	2016-11-06T15:00:00	2017-05-09T16:30:00	206	16	100
F3B08	RBR#60335	47.579797	-55.168053	2016-11-06T15:00:00	2017-05-09T16:30:00	206	88	100
F3B08	UTBIs	47.579797	-55.168053	2016-11-06T15:00:00	2017-05-09T16:30:00	206	17-79	100
F3B11	WH300#11351	47.478673	-55.165868	2016-11-05T17:25:00	2017-05-09T15:13:00	98	87	99
F3B11	SBE37#14433	47.478673	-55.165868	2016-11-05T17:25:00	2017-05-09T15:13:00	98	16	100
F3B11	SBE37#14434	47.478673	-55.165868	2016-11-05T17:25:00	2017-05-09T15:13:00	98	88	100
F3B11	UTBIs	47.478673	-55.165868	2016-11-05T17:25:00	2017-05-09T15:13:00	98	17-79	100
F3B12	WH1200#13990	47.712317	-55.416800	2016-11-04T13:22:00	2017-05-11T10:43:00	10	8	112
F3B12	SBE37#14436	47.713567	-55.418317	2016-11-05T12:00:00	2017-05-11T11:05:00	8	3	100
F3B12	SBE37#14435	47.712317	-55.416800	2016-11-04T13:22:00	2017-05-11T10:43:00	10	8	100

Table B-5: Land-based data collection summary along the whole program (May 2015 – May 2017)

Site	Instrument	Latitude (ºN)	Longitude (ºW)	Deployment	Recovery	Site Depth	Instrument Depth	% Coverage
DOGIS	SUTRON#1204160	47.61463	-55.35221	2015-05-04T16:50:00	2015-10-15T16:25:00	-10	-20	92
DOGIS	SUTRON#1204160	47.61463	-55.35221	2015-10-15T16:30:00	2015-11-19T17:00:00	-10	-20	100
DOGIS	SUTRON#1204160	47.61463	-55.35221	2015-11-19T17:30:00	2016-05-14T13:30:00	-10	-20	98
DOGIS	SUTRON#1204160	47.61463	-55.35221	2016-05-14T13:50:00	2016-11-03T12:30:00	-10	-20	99
DOGIS	SUTRON#1204160	47.61463	-55.35221	2016-11-03T15:20:00	2017-01-19T12:30:00	-10	-20	56
DOGIS	SUTRON#1204160	47.61463	-55.35221	2017-01-19T13:40:00	2017-05-09T18:00:00	-10	-20	98
DOGIS	U30#10072354	47.61463	-55.35221	2015-05-03T19:00:00	2015-11-19T18:05:00	-10	-12	96
DOGIS	U30#10072354	47.61463	-55.35221	2015-11-19T18:30:00	2016-05-14T12:00:00	-10	-12	83

DOGIS	U30#10072354	47.61463	-55.35221	2016-05-14T12:30:00	2016-06-14T15:40:00	-10	-12	100
DOGIS	U30#10072354	47.61463	-55.35221	2016-06-14T16:00:00	2016-11-03T12:30:00	-10	-12	87
DOGIS	U30#10072354	47.61463	-55.35221	2016-11-03T15:50:00	2017-01-19T14:30:00	-10	-12	99
DOGIS	U30#10072354	47.61463	-55.35221	2017-01-19T14:40:00	2017-05-09T18:00:00	-10	-12	99
DOGIS	U20#10305631	47.61463	-55.35221	2015-05-03T19:00:00	2015-11-19T18:05:00	-10	-12	100
DOGIS	U20#10305631	47.61463	-55.35221	2015-11-19T18:19:00	2016-05-14T14:00:00	-10	-12	100
DOGIS	U20#10305631	47.61463	-55.35221	2016-05-14T15:00:00	2016-11-03T12:30:00	-10	-12	100
DOGIS	U20#10305631	47.61463	-55.35221	2016-11-03T16:15:00	2017-05-09T18:30:00	-10	-12	100
POOLC	SUTRON#1112700	47.67993	-55.43002	2015-05-01T18:40:00	2015-11-19T22:00:00	3	2	100
POOLC	SUTRON#1112700	47.67993	-55.43002	2015-11-19T22:10:00	2016-05-15T12:00:00	3	2	73
POOLC	SUTRON#1112700	47.67993	-55.43002	2016-05-15T13:10:00	2016-11-04T10:48:24	3	2	99
POOLC	SUTRON#1112700	47.67993	-55.43002	2016-11-04T11:00:00	2017-05-11T14:00:00	3	2	54

Table B-6: IFREMER data collection summary

Site	Instrument	Latitude (ºN)	Longitude (ºW)	Deployment	Recovery	Site Depth	Instrument Depth	% Coverage
SPMGF	WH300	46.9581	-56.2293	2015-06-22T13:11	2015-09-15T16:51	78	77.5	98
SPMGF	WH300	46.9581	-56.2293	2015-09-18T13:08	2015-11-18T18:58	81	80.5	86
SPMGF	WH300	46.9581	-56.2293	2016-03-18T13:04	2016-05-30T17:54	81	80.5	87
SPMGF	WH300	46.9581	-56.2293	2016-06-02T17:04	2016-11-15T16:24	79	78.5	98
M01	MASTODON#03070	46.9880	-55.9900	2016-05-22T12:00	2016-10-30T00:00	60	60	100
M02	MASTODON#03081	47.1780	-56.1390	2016-05-22T12:00	2016-10-30T00:00	60	60	100
M03	MASTODON#03089	47.0700	-55.8800	2016-05-22T12:00	2016-10-30T00:00	60	60	100
M05	MASTODON#03066	47.1250	-55.770	2016-05-22T12:00	2016-10-30T00:00	60	60	100
M06	MASTODON#03062	47.2400	-55.870	2016-05-22T12:00	2016-10-30T00:00	60	60	100
M07	MASTODON#03077	46.8250	-56.1667	2016-07-13T20:00	2016-10-30T00:00	60	60	100
M08	MASTODON#03041	46.8667	-56.1833	2016-07-13T20:00	2016-10-30T00:00	60	60	100
M09	MASTODON#03051	46.9500	-56.1833	2016-07-13T20:00	2016-10-30T00:00	60	60	100
M10	MASTODON#03046	47.0250	-56.1533	2016-07-13T20:00	2016-10-30T00:00	60	60	6
M11	MASTODON#03060	47.0917	-56.1667	2016-07-13T20:00	2016-10-30T00:00	60	60	100
M12	MASTODON#03067	47.1250	-56.2833	2016-07-13T20:00	2016-10-30T00:00	60	60	100

595